ELSEVIER

Surface Science 345 (1996) 320–330

surface science

Detecting stacking faults during epitaxial growth by low energy electron diffraction

H. Ascolani [a], J.R. Cerda [a], P.L. de Andres[a,*], J.J. de Miguel [b], R. Miranda [b], K. Heinz [c]

[a] *Instituto de Ciencia de Materiales (CSIC), Cantoblanco, E-28049 Madrid, Spain*
[b] *Dartamento Fisica de la Materia Condensada, C-III, Universidad Autonoma, E-28049 Madrid, Spain*
[c] *Lehrstuhl für Festkörperphysik, Universität Erlangen-Nürnberg, Staudtstrasse 7, D-91058 Erlangen, Germany*

Received 18 January 1995; accepted for publication 28 August 1995

Abstract

We study the sensitivity of LEED to stacking faults in the early stages of epitaxial growth. By theoretical simulation of stacking faults in different locations, in particular for Cu/Cu(111), Co/Cu(111), and p(4 × 4)Pb/Cu/Cu(111), we show that quantitative LEED can detect stacking faults down to three or four layers deep into the substrate. This is also true in the presence of a surfactant layer. The modification of the intensity spectra by stacking faults is large enough to be identified by visual comparison with defect-free surfaces. In the cases where different stacking sequences coexist on the surface, a minimum coverage of 30%–50% imperfect stacking sequences is needed in order to be clearly detected in the LEED *I–V* curves. Therefore, our results provide guidance to conduct experiments where early detection of stacking faults is important.

PACS: 68.35.B; 61.72.N; 68.55; 83.70

Keywords: Cobalt; Copper; Electron–solid interactions, scattering, diffraction; Growth; Low energy electron diffraction (LEED)

1. Introduction

The epitaxial growth of metals on metals is a topic that has received sustained attention for many years. The case of a magnetic metal deposited on a non-magnetic metallic single crystal has attracted fundamental and technical interest in the past few years triggered by the discovery of phenomena related to the reduced symmetry of the thin film, such as perpendicular anisotropy [1], thickness-dependent Curie temperatures [2], modified critical exponents [3], oscillatory magnetic coupling [4] and spin-polarized quantum well states [5,6]. A simple energetic consideration indicates that these magnetic properties are expected to be strongly modified by the structure of the films, since magnetic energies are vastly inferior to bonding energies. The latter can be modified changing the structure by epitaxial growth. So, e.g., lattice parameters may be changed with respect to their bulk counterparts by pseudomorphic growth [7], metastable phases (e.g. fcc Co) can be stabilized in a different temperature region by growth onto suitable substrates [8], and even new phases (e.g. bcc Co) may be found [9].

In order to understand and control the resulting magnetic properties of novel artificial structures, a detailed structural characterization of the grown films is needed. For such a task, the application of

* Corresponding author.

SSDI 0039-6028(95)00881-0

complementary experimental techniques is very useful, such as scanning tunneling microscopy (STM), low-energy electron diffraction (LEED) and X-ray diffraction at grazing incidence. In particular, it is necessary not only to characterize the average film but also to be able to recognize the different kinds of defects, since in many cases they control the growth and the magnetic properties of the film. A relevant problem involves the growth of magnetic metals on fcc substrates with (111) orientation, where there are two adsorption sites of three-fold symmetry, whose energies are not expected to be much different [10]. The incoming atoms could then nucleate on both of these sites, resulting in stacking faults which could lead to twinning or varying sequences of stacking as the growth of the film proceeds. It has to be noted that stacking faults are among the defects with the least energetic cost for fcc metals, with values ranging from 80 to 300 erg/cm^2 (50–180 meV/atom) [11]. The existence of a stacking fault in the early stages of the growth is not easy to infer from the data obtained with most structural techniques. Its identification is, however, essential, since the existence of stacking faults determines whether the film is continuous, twinned or otherwise imperfect.

At first sight, dynamical LEED [12–15] seems to be an ideal technique to study these problems. The strong elastic interaction between electrons and the atoms forming the surface results in extreme sensitivity to the atomic positions, as has been extensively demonstrated over the past years on many accurate surface-structure studies. The inelastic interaction, which is also strong, limits the scope of the technique to the vicinity of the surface, but this is precisely the region that matters for growth processes. Finally, from a practical point of view, only standard, inexpensive equipment, already forming part of most ultra-high vacuum systems for surface studies, is needed. In spite of this, LEED has not been used, as far as we know, to study the above-mentioned problems. Previous attempts to detect stacking faults in homoepitaxy using LEED [16] have involved the analysis of the spot profiles. However, the sensitivity achieved is much lower than that we present in the following by I–V curves. We show that the analysis of the I–V curves of diffraction spots in LEED is an extremely sensitive tool to detect the presence of stacking faults in the epitaxy of metals on metals. We have carried out multiple scattering calculations producing I–V curves for a number of situations possibly realized in the experiment. In Sections 1 and 3, we analyze the appearance of stacking faults in the homoepitaxial growth of Cu on Cu(111) and in the heteroepitaxial growth of Co on Cu(111), respectively. In Section 4, we address the effects of surfactant adsorbed layers on the LEED sensitivity to stacking faults, by performing a detailed study of the system p(4×4)Pb/Cu/Cu(111), besides other hypothetical overlayers of Sb or As.

2. Homoepitaxy

As a first demonstration of the capabilities of LEED to detect stacking faults during homoepitaxy, we have analyzed the sensitivity of the I–V curves to the presence of stacking faults in the first five layers of a Cu(111) crystal. On top of a perfect Cu(111) crystal (ABCABC stacking) we have placed five Cu layers with all possible stacking sequences leading to a total of $2^5=32$ test structures. No surface reconstruction was considered, so that p(1×1) symmetry is assumed throughout this section. Furthermore, all structures preserve the symmetry of the clean surface, namely a three-fold axis plus a mirror plane. Full dynamical calculations were performed for each structure choosing standard and simple conditions as normal incidence of the primary beam and room temperature. The non-structural parameters defining the Cu surface are as follows: $\Theta_{\mathrm{Debye}}=330$ K, $V_{0\mathrm{r}}=-12$ eV, $V_{0\mathrm{i}}\propto E^{1/3}$, and the phase shifts are obtained from the MUFPOT program [12]. All interlayer spacings were set equal to that of bulk Cu(111). We have calculated the spectra of six symmetry-inequivalent beams ((00), (01), (10), (11), (02), and (20)) for a typical energy range 50–300 eV. The (00) beam was calculated in order to determine its sensitivity to stacking faults, but it was not included in the evaluation of the averaged R-factors because it cannot be measured under the usual condition of normal incidence.

We start by illustrating in Fig. 1 and Fig. 2 the sensitivity of the I–V curves to a single stacking fault located at different depths. In both figures, the curve at the bottom corresponds to a perfect fcc stacking. The other four curves correspond to imperfect growth with one stacking fault located in the fourth layer, third layer, second layer and first layer, respectively. As expected, the differences between these I–V curves and the fcc curve increase as the stacking fault comes closer to the surface. Both for the (10) and the (01) beams, it becomes clear by visual inspection that stacking faults located at depths less or equal to three layers yield

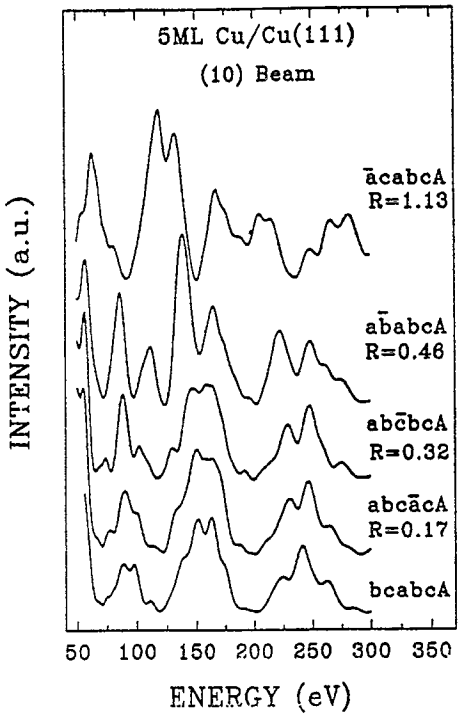

Fig. 1. Intensity spectra of the (10) beam at normal incidence for 5 ML Cu/Cu(111). The I–V curves correspond to different stacking sequences of the first five Cu layers. The curve at the bottom corresponds to a perfect fcc stacking, and the other curves to stacking sequences with a single stacking fault located at different depths. The corresponding stacking sequences are shown on the right. Lower-case letters indicate the stacking of the five Cu layers deposited, and the upper-case letter gives the stacking of the first layer of the fcc Cu(111) crystal (ABCABC... stacking). The bar indicates the position of the stacking fault. The numbers below the stacking sequences correspond to the Pendry R-factors between each curve and the perfect fcc stacking one.

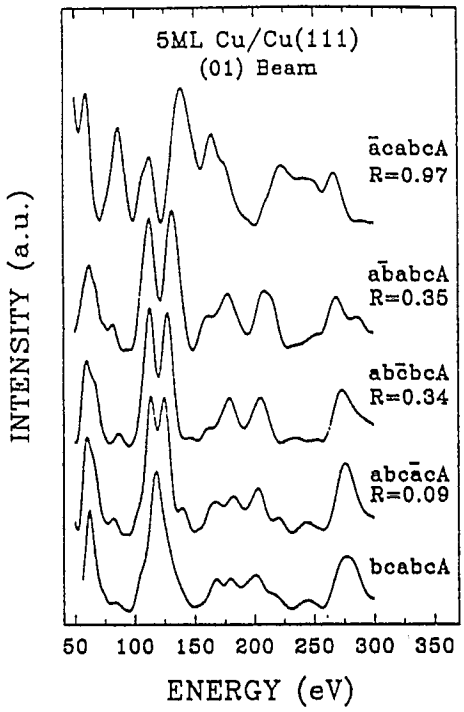

Fig. 2. Same as in Fig. 1, but for the (01) beam.

spectra significantly different from the reference. This clearly demonstrates the capability of LEED to detect defects in the fcc stacking order.

In order to investigate to what extent the above findings can be generalized to other structures, we chose two extreme structures as references: a perfect Cu(111) crystal and a system consisting of 5 ML of Cu stacked in an hcp sequence on top of the Cu(111) (i.e. bababABC... stacking). We have then compared the spectra calculated for each of these two references with those corresponding to the remaining 31 structures. We chose the commonly used reliability factor defined by Pendry (R_P) [17] to quantitatively compare between the reference and each structure. For both references, we find that the R-factor values are dominated by the location of the topmost stacking fault, with much less influence of the stacking underneath. For instance, let us consider the case of the fcc reference (bcabcABC stacking). The eight structures with the last stacking fault in the second layer yield Pendry R-factors between 0.52 and 0.60(these values correspond to the structures abācaBCA and abābaBCA, respectively). As we

want to determine which structures are distinguishable from the reference and which are not, we have included in Table 1 only those structures which yield the lowest Pendry R-factor for each position of the first stacking fault. Table 1 reveals that the general trend of the R-factor is to increase as the first stacking fault approaches the surface, in agreement with the evolution of the I–V curves shown in Figs. 1 and 2. By comparing the R-factors obtained with one reference and the other for the same position of the first stacking fault, it is clear that it is easier to detect stacking faults in fcc than in hcp structures. Taking into account that the agreement between experimental and theoretical I–V curves is considered good when they differ in a Pendry R-factor lower than 0.20, we consider larger values sufficient to distinguish between different spectra. So, we conclude that LEED can easily detect deviations from the fcc (hcp) stacking sequence up to the third (second) layer. Notice that this conclusion, which results from the analysis of the R-factors, agrees with that derived from Figs. 1 and 2 by simple visual comparison of the I–V curves.

This result for the sensitivity of LEED to stacking faults is consistent with the estimated depth sensitivity given by $\lambda_e/(2\alpha_\perp)$, where λ_e is the inelastic mean free path for the electron wave and $\alpha_\perp$ the interlayer distance. In our calculations we set λ_e to $\sim$12 Å at 200 eV and the interlayer distance $\alpha_\perp$ to 2.087 Å, resulting an expected depth sensitivity of $\sim$3 monolayers. We have evaluated the sensitivity to stacking faults different hypothetical values of λ_e in the system Cu/Cu(111), and we have found in all the cases that it is approximately given by the ratio $\lambda_e/(2\alpha_\perp)$. Therefore, we expect that in the epitaxial growth of metals on the surface (111) of fcc metals, the LEED technique will be able to detect stacking faults located in the first $\lambda_e/(2\alpha_\perp)$ monolayers.

Table 1
Pendry R-factors for different positions of the last stacking fault; the position of the last stacking fault is indicated by a bar

Stacking order	Position of the last stacking fault	Pendry R-factors
abcabABC...		fcc reference
abcācBCA...	4th layer	0.14
abc̄baCAB...	3rd layer	0.37
ab̄acaBCA...	2nd layer	0.52
ācabcABC...	1st layer	0.93
bababABC...		hcp reference
babācABC...	4th layer	0.04
bab̄cbABC...	3rd layer	0.18
bācabCAB...	2nd layer	0.54
b̄cbcaCAB...	1st layer	0.50

Regarding the sensitivity of individual beams to stacking faults, we have found that the (11) beam has greater sensitivity than the other beams when two non-twinned structures are compared (twinning reducing this sensitivity due to the six-fold symmetry). As illustrated in Figs. 4, 5 and 6, the contribution of the (11) beam to the averaged R-factor complements those of the (10) and (01) beams in a decisive way. Thus, the minimum set of beams necessary to discriminate between the 31 structures is that formed by the (01), (10) and (11) beam. The (20) and (02) beams behave similarly to the (10) and (01) beams. The case of the (00) beam, not included in the calculation of the averaged R-factors in Table 1 and Table 2, is interesting because it feels the stacking sequences mainly through multiple scattering effects. This beam yields Pendry R-factors of 0.52, 0.79, 0.58, 0.20 between structures with one, the stacking fault in the first, second, third and fourth layer, respectively, and the perfect fcc stacking. These values show the considerable sensitivity of this beam.

In the analysis presented above, we have considered the case where one particular stacking sequence perfectly covers all the surface. However, as the energy needed to create a stacking fault is small and as a consequence of homogeneous nucleation, it is likely that domains with different stacking sequences could coexist on the surface. In order to determine the minimum amount of imperfect growth that can be detected by LEED, we have considered the case where the fcc stacking sequence coexists on the surface with a particular imperfect sequence. We assume that the dimensions of the domains are big enough so the I–V curves can be obtained by taking weighted averages of the intensities calculated for the two stacking sequences. As shown in Fig. 3, imperfect stacking sequences with a stacking fault in the first, second and third layer

Table 2
Pendry R-factors for different positions of the last stacking fault for several hypothetical surfactant overlayers are shown in columns 3 to 6; in the seventh column appears the averaged Pendry R-factor between the (10), (01), (11), (20) and (02) beams of each superstructure and those of the fcc Cu(111)

Superstructure on Cu(111)	Coverage θ	O–ācabcABC	O–ab̄acaBCA	O–abc̄baCAB	O–abcācBCA	R_P
p(1×1)As	1	0.59	0.44	0.14	0.08	0.36
p(1×1)Pb	1	0.60	0.52	0.16	0.09	0.81
p(4×4)Pb	9/16	0.90	0.54	0.32	0.08	0.26
p(4×4)Pb buckled	9/16	0.84	0.46	0.28	0.06	0.32
p(2×2)Sb	1/2	0.79	0.41	0.29	0.11	0.60
$(\sqrt{3}\times\sqrt{3})$R30° Pb	1/3	0.82	0.53	0.32	0.18	0.45
$(\sqrt{3}\times\sqrt{3})$R30° Sb	1/3	0.80	0.50	0.30	0.14	0.36
P(2×2)Pb	1/4	0.89	0.53	0.34	0.18	0.32
p(2×2)Sb	1/4	0.84	0.54	0.32	0.15	0.40

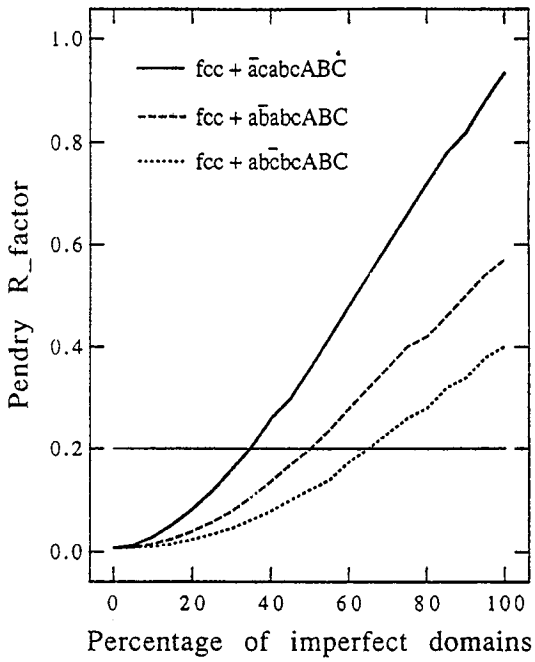

Fig. 3. R-factor between I–V curves calculated for a system where domains with the perfect fcc stacking and imperfect stacking sequences coexist.

are clearly detected for coverages greater than 35%, 50% and 65%, respectively.

Therefore, we propose as a straightforward way to monitor homoepitaxy of fcc metals onto (111) surfaces, to measure the LEED I–V curves after deposition of at most two monolayers. Then they can be compared visually with those measured for a substrate known to be free of stacking faults near the surface or just with standard full dynamical calculations. If the I–V curves of the studied system are very similar to those of the substrate, at least a 50%–70% of the surface presents the perfect fcc stacking sequence. On the contrary, if the existence of defects is detected in the I–V curves, they should be compared with the I–V curves corresponding to each one of the possible stacking sequences. From this comparison, it could be determined which particular imperfect sequence is dominant. Finally, if the experiment cannot be fitted with I–V curves corresponding to single stacking sequences or with a weighted average of them, it can be concluded that stacking faults are not the most important kind of defect occurring on the surface. From a practical point of view it would be useful to prepare a data base of experimental I–V curves for known references and calculated I–V curves corresponding to different stacking sequences for a variety of fcc metals.

We stress that no particular attempt to optimize the sensitivity was made (e.g. choosing the most sensitive beams or a particular energy range). Therefore, we expect these results to be relevant for a wide range of homoepitaxial systems of metals on fcc (111) surfaces, such as Cu/Cu(111) [18], Ag/Ag(111) [19], or Pt/Pt(111) [20].

3. Heteroepitaxy

It is also important to determine the stacking sequence during heteroepitaxial growth. Thus, the development of stacking faults could be a mecha-

nism to reduce the strain in the film, e.g. Ag/Pt(111) [21], to modify the orientation of the magnetization, e.g. in Co/Au(111) [22], or a way for the fcc to hcp structural phase transition to occur [23].

In cases such as Co/Cu(111) [24], the film structure evolves from fcc to hcp [25] and the evolution is mediated by stacking faults being introduced into the film. The presence of the fcc or hcp stacking has important consequences for the mode of growth of Co/Cu multilayers [26].

In order to asses the capabilities of LEED regarding this problem, we have calculated the *I–V* curves for the eight different possibilities of stacking three monolayers of Co on Cu(111), but did not take into account the possible existence of different domains. For Co we have used Θ_{Debye} = 385 K, while retaining all other parameters at the same values as in the previous section. The calculated *I–V* spectra for (10), (01) and (11) beams are shown in Fig. 4, Fig. 5, and Fig. 6, respectively. We have organized these figures in such a way that similar spectra appear consecutively, in order to facilitate visual comparison. The corresponding stacking sequences are illustrated in the figures, as well as the *R*-factor values between consecutive curves.

There are four pairs of twinned structures (e.g. 1 and 8 or 4 and 5). For any given structure, the (10) spectrum is very similar to the (01) data of the corresponding twin structures, as illustrated in Figs. 4 and 5. The calculated *I–V* spectra for the (11) diffracted beam are reproduced in Fig. 6. Due to the intrinsic six-fold symmetry of the (11) beam it lacks sensitivity to the twinning of the structure, while it can distinguish between different locations of the stacking fault more reliably than (10) or (01) beams. Then, we conclude that the eight

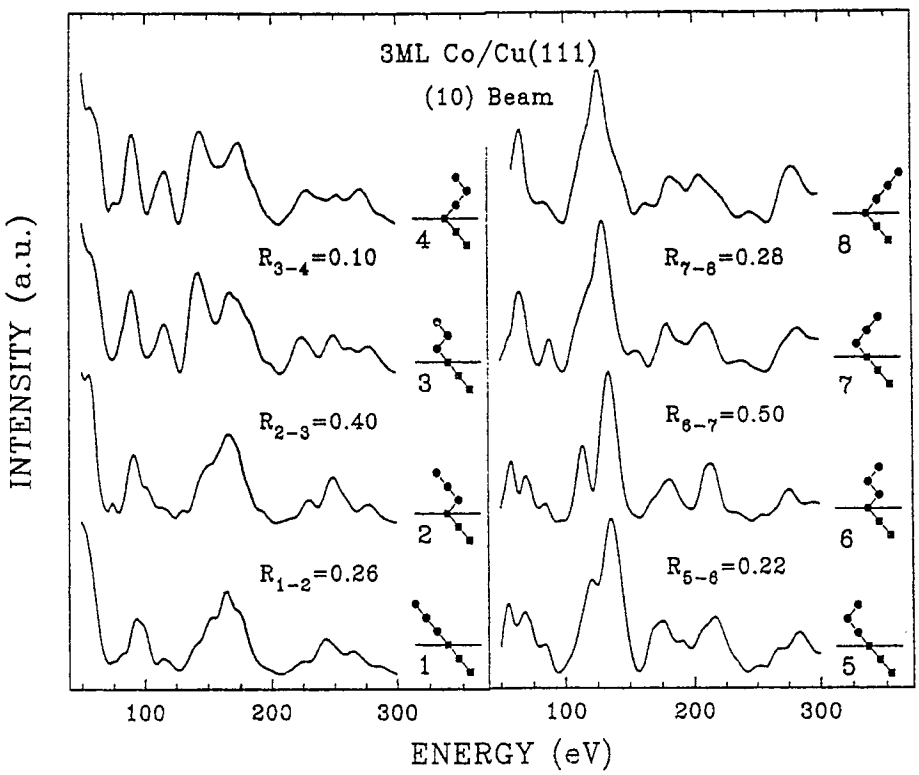

Fig. 4. Intensity spectra of the (10) beam at normal incidence for the eight different possibilities of stacking of 3 monolayers of cobalt deposited on Cu(111). For each structure, the stacking sequence is shown in the inset on the right. The squares represent the fcc stacking of the substrate (ABCABC...) and the circles that of cobalt layers. The Pendry *R*-factors between consecutive structures are indicated.

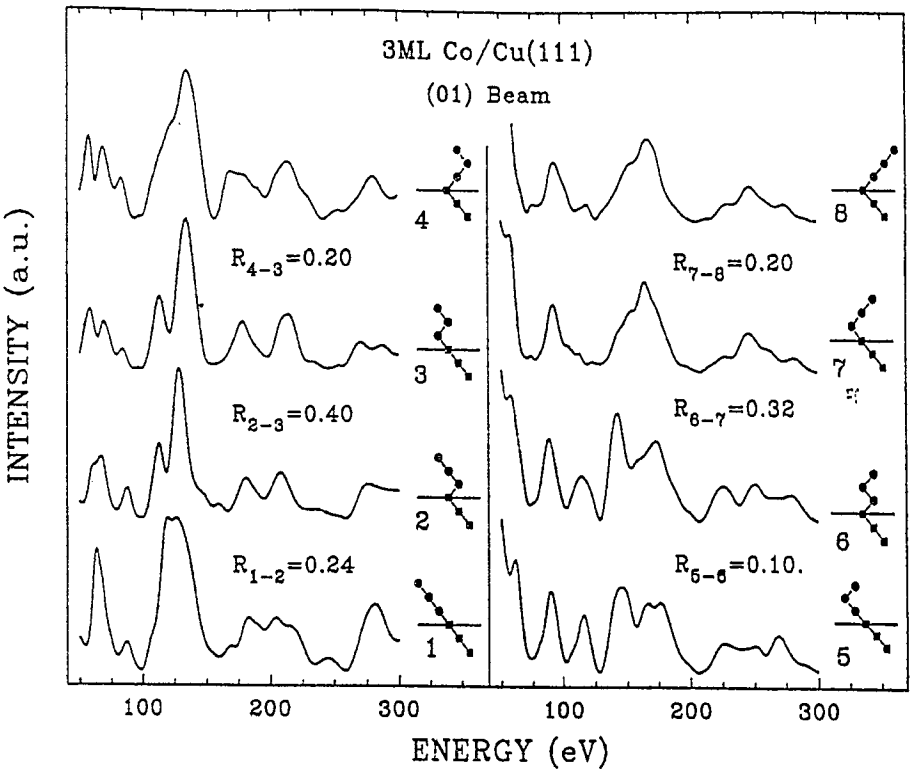

Fig. 5. Same as in Fig. 3, but for the (01) beam.

different possibilities to accommodate the three cobalt layers can be discriminated combining the comparative analysis of the I–V curves for these three beams. It is clear that this conclusion is obtained best by using the R-factor analysis, but also by direct visual inspection.

It is important to point out that the differences between the fcc I–V curves for Co/Cu(111) and those for Cu/Cu(111) are smaller than the variations in the I–V curves produced by the presence of a stacking fault anywhere in the cobalt trilayer. Therefore, the experimental I–V curves for the Cu(111) substrate could be used as a reference for the fcc stacking in order to monitor the growth mode.

4. Surfactants

As first suggested by Cabrera and Vermilyea [27] in 1958, the mode of growth of a given film can be modified by depositing a layer of a different material (surfactant) on the surface of the substrate. It modifies the film growth either by the energetics or the kinetics or both. In the case of metals, it has been reported that the modes of growth of Ag/Ag(111) [19] and Pt/Pt(111) [20] are modified from three-dimensional growth to a layer-by-layer mode by using Sb or O as surfactants. For O/Pt/Pt(111) the LEED pattern was p(2×2) with sharp LEED spots [20], but no LEED I–V curves were reported. In no case was a complete surface structure determination attempted, so the adsorption positions for the surfactants in the growing layers are unknown. Possibly, the position of O on Pt/Pt(111) is the same as on Pt(111), i.e. three-fold hollow sites as recently determined by LEED [28].

A particularly interesting surfactant effect has been recently reported for Pb/Cu(111) [29]. Co/Cu superlattices grown on Cu(111) show twinning of the Cu spacer layers, which produces islands of different orientations (twins) that do not coalesce. Because of the direct ferromagnetic cou-

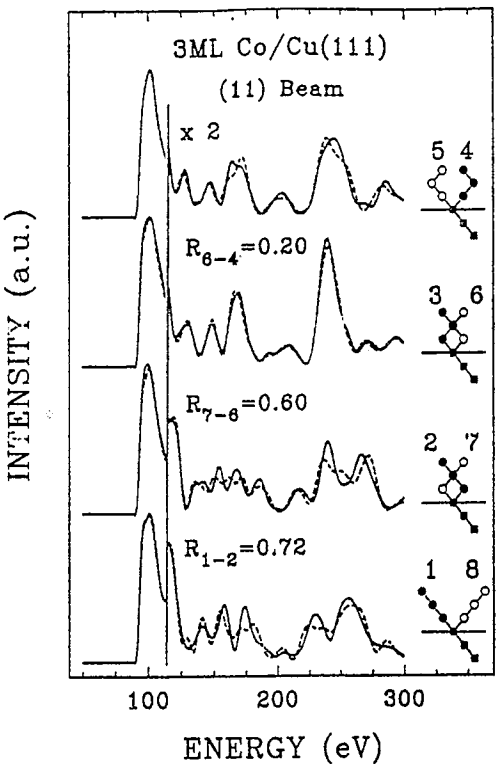

Fig. 6. Same as in Fig. 3, but for the (11) beam. The *I–V* curves corresponding to twinned structures have been superimposed. The continuous lines correspond to the structures represented with filled circles in the inset, and the dashed ones to the strutures represented by open circles.

pling between adjacent Co layers, the twinning of the growing layers and the associated lack of lateral continuity might be responsible for the lack of antiferromagnetic coupling and the related giant magnetoresistence in (111)-oriented Co/Cu superlattices grown by MBE [30]. This problem has confused researchers in this field during the last years. The predeposition of a layer of Pb on the Cu(111) surface prior to the Co/Cu growth suppresses twinning in the intermediate Cu layers [29]. Contrary to the Sb/Ag(111) system where Sb is continuously lost [19], it has been experimentally observed that the p(4×4) superstructure characteristic of the Pb overlayer persists during the growth of Cu/Co sandwiches, which is a strong indication of Pb floating on top of the deposited layers [29]. Another case where the surfactant results in a persisting LEED superstructure pattern was the p(2×2) O/Pt(111) [20], where it is equally suggested that the surfactant floats analogously to the Pb case.

Adding a surfactant might be a way to improve epitaxial growth but could possibly make the analysis of the stacking sequence of the system more difficult. In order to check for that, we have performed an analysis for p(4×4)Pb/Cu/Cu(111) similar to that described above for Cu/Cu(111). The structural model used for the p(4×4)Pb overlayer is a perfect hexagonal lattice with a lattice constant equal to 4/3 of that of the Cu(111) surface lattice. Therefore, there are nine Pb atoms per unit cell. The surfactant layer is placed on top of the fcc Cu(111) crystal, thus forming an O–abcabCAB... stacking, where O– denotes the surfactant layer. According to a hard sphere model, one Pb atom is located at an fcc site, another atom at an hcp site, another atom at a top site, and the other six atoms occupy asymmetrical sites. A full dynamical LEED calculation was performed for this system, and the resulting spectra were used as reference. Next, we introduced all possible stacking faults in the first five layers of the Cu crystal. This amounts to $2^{(5-1)}=16$ structures, whose spectra were compared with the reference again by means of the Pendry *R*-factor, R_P. Relativistic phase shifts obtained with MUFPOT and a Debye temperature of 100 K were used for Pb. The registry of the overlayer relative to the top Cu layer (O–a...) was always kept constant, since it is not the surfactant adsorption site which is analyzed here, but the substrate stacking sequence.

The effect of the surfactant overlayer on the LEED spectra can be evaluated comparing the results obtained for p(4×4)Pb/Cu/Cu(111) with those of Cu/Cu(111). In Fig. 7 we show the *I–V* curves of the (10) beam for the p(4×4)Pb which are in correspondence with those presented in Fig. 1. In Fig. 7 the lower curve corresponds to a Pb overlayer deposited on a perfect fcc Cu(111) crystal; next, the curve corresponding to the structure with one stacking fault in the fourth Cu layer (O–abcācABC... stacking) is shown, and so on. Comparing these spectra with those of Fig. 1, we surprisingly find that they are rather similar. If we consider that the overlayer has the maximum possible coverage and that Pb is a heavy atom, the effect of the p(4×4)Pb overlayer on the integer beams is much less than expected. Furthermore,

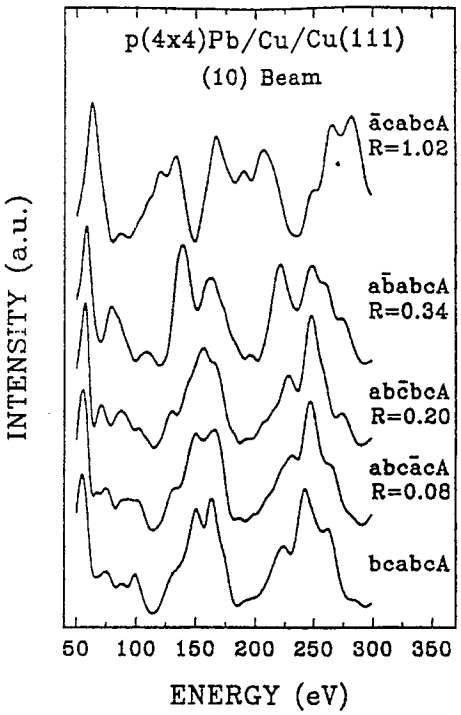

Fig. 7. Same as in Fig. 1, but for the p(4×4)Pb/5 ML Cu/Cu(111). The stacking sequence of the substrate are shown on the right. The registry of the Pb overlayer relative to the top Cu layer has been kept constant.

since the integer beams are only slightly perturbed by the surfactant overlayer, their sensitivity to the stacking order of the substrate is practically unaltered. This can be observed in Fig. 7 by comparing curves corresponding to different positions of the stacking fault with the pure fcc spectrum.

The same conclusion is derived by quantitative analysis as shown in Table 2. The Pendry *R*-factors in columns 3 to 6 are comparable with those presented in the upper panel of Table 1 (fcc reference), being practically the same. In the seventh column it is found the averaged Pendry *R*-factor between the integer beams of the p(4×4)Pb and those of the fcc Cu(111). Therefore, we can conclude that the p(4×4)Pb overlayer does not obscure the LEED analysis of the stacking order underneath. Furthermore, the *I–V* curves measured on the Cu(111) could be used as reference of fcc stacking to monitor the epitaxial growth of Cu/Co multilayers on Cu(111) even in the presence of Pb on top of the deposited layers.

One possible reason for the weak influence of the Pb overlayer on the substrate beams is due to the fact that the Pb overlayer forms an hexagonal Bravais lattice with a lattice constant being 4/3 that of the Cu. This results in overlayer diffraction matrix coupling to the integer-order beams being very small. To test the relevance of this mere geometrical factor, we have also considered several different buckled reconstructions for the Pb layer including atomic displacements up to 0.4 Å. In this case, all matrix elements become nonzero, but the result of the *R*-factor comparison yield only a small reduction on the LEED sensitivity to the last stacking fault location (see *R*-factor values in Table 2). At the same time, an increment of the *R*-factor respect to the clean fcc Cu(111) from 0.26 to 0.32 is observed. Also, the effect of temperature was analyzed: We have calculated the Pendry *R*-factors for the spectra corresponding to the p(4×4) at 0 K to find that it is in the order of ~10% with respect to the room temperature results, showing that thermal vibrations are not relevant to our conclusions.

In order to investigate to what extent the behaviour of the p(4×4)Pb is valid for other surfactant overlayers, we have repeated the analysis for several hypothetical superstructures of Pb, Sb, and As, deposited on Cu(111). They are listed in the first column of Table 2 and their corresponding coverages in the second column of this table. Coverage has been defined as the ratio of the number of surfactant atoms to the number of substrate atoms. Despite the p(1×1)Pb being unrealistic, it was included in the analysis in order to scan a wide range of coverages with Pb, which as a heavy atom is expected to produce pronounced effects in the p(1×1) arrangement. Table 2 shows that the Pendry *R*-factors obtained by stacking sequences with the first stacking fault in the first or in the second layer of the substrate (third and fourth column in the table) are large enough to safely discriminate from the pure fcc reference (notice that we have assumed that a Pendry *R*-factor lower than 0.2 for a stacking sequence indicates that it cannot be discriminated from the reference). *R*-factors obtained from stacking sequences with the first stacking fault in the third layer (fifth column) exhibit a strong decrease only for the high coverage p(1×1)As and p(1×1)Pb

overlayers. Surfactant overlayers with coverages below about 0.5 ML, on the other hand, do not significantly alter the sensitivity of LEED to stacking faults. As this result is obtained for several superstructures of Pb and Sb, two heavy atoms, we expect it to hold also for superstructures of lighter surfactants such as O or CO. The R-factors in the seventh column of Table 2 indicate that when surfactants are used it is generally not valid to use the I–V curves of the substrate as reference of perfect fcc growth, although exceptional cases like the case of the p(4×4)Pb can be found.

Finally, we have considered the case of the surfactant obscuring the stacking sequence in heteroepitaxial growth. I–V curves for a p(4×4)Pb/2 ML Co/Cu(111) structure have been calculated for the four different stacking possibilities of the cobalt layers. The results are displayed in Fig. 8. Clearly, all structures can be discriminated in spite of having the Pb overlayer at the external surface.

5. Conclusions

In conclusion, we have demonstrated the potential of dynamical LEED studies with respect to the quantitative detection of stacking faults appearing during the growth process of epitaxial films. The sensitivity is such that buried defects up to the third or fourth layer can easily be detected under normal experimental conditions by simple visual inspection of the measured I–V curves. We have also evaluated the cases where different stacking sequences coexist on the surface. A minimum of 30%–50% of the surface with imperfect stacking sequences is needed in order to clearly detect the

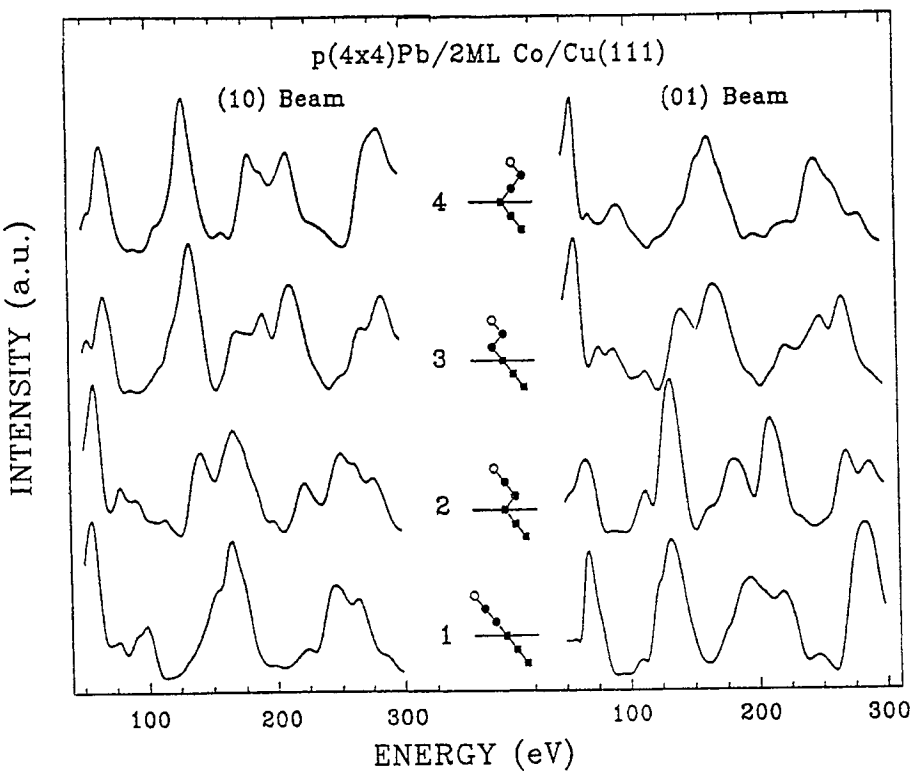

Fig. 8. Intensity spectra of the (10) and (01) beams at normal incidence for the p(4×4)Pb/2 ML Co/Cu(111). The open circles in the insets represent the stacking of the Pb overlayer.

presence of these defects by means of the LEED I–V curves. To illustrate the situation, we have performed a number of calculations on interesting systems such as Cu/Cu(111), Co/Cu(111), and p(4×4)Pb/Cu/Cu(111). We have also analyzed the effect of surfactant coverages on the LEED sensitivity with respect to stacking faults. We find that it is negligible for coverages lower than 0.5 independently of which surfactant is used. On the other hand, for coverage of about 1, the sensitivity to identify a stacking fault is reduced by one layer.

Acknowledgements

This work has been partially financed by the Spanish CICYT (contract number PB91-0930). We are also grateful to the German Research Foundation (DFG) and the *Acciones Integradas* program (DAAD) for further support. H. Ascolani acknowledges a post-doctoral grant from the Spanish Ministry of Education and Science, and partial support from the Consejo Nacional de Investigaciones Cientificas y Técnicas of Argentina.

References

[1] J.G. Gay and R. Richter, Phys. Rev. Lett. 56 (1986) 2728.
[2] C.M. Schneider et al., Phys. Rev. Lett. 64 (1990) 1059.
[3] F. Huang, M.T. Kief, G.J. Mankey and R.F. Willis, Phys. Rev. B 49 (1994) 3962.
[4] J.J. de Miguel et al., J. Magn. Magn. Mater. 93 (1991) 1.
[5] J.E. Ortega and F.J. Himpsel, Phys. Rev. Lett. 69 (1992) 844.
[6] C. Carbone et al., Phys. Rev. Lett. 71 (1993) 2805.
[7] J.R. Cerda, P.L. de Andres, A. Cebollada, R. Miranda, E. Navas, P. Schuster, C.M. Schneider and J. Kirschner, J. Phys. Condens. Matter 5 (1993) 2055.
[8] L. Gonzales, R. Miranda, M. Salmeron, J.A. Verges and F. Yndurain, Phys. Rev. B 24 (1981) 3245.
[9] G. Prins, Phys. Rev. Lett. 54 (1985) 1051.
[10] B. Piveteau et al., Phys. Rev. B 46 (1992) 7121; C.L. Liu et al., Surf. Sci. 253 (1991) 334.
[11] F. Yndurain and L.M. Falicov, Phys. Rev. Lett. 37 (1976) 928.
[12] J.B. Pendry, Low Energy Electron Diffraction (Academic Press, London, 1974).
[13] M.A. Van Hove and S.Y. Tong, Low Energy Electron Diffraction (Springer, Berlin, 1979).
[14] K. Heins, Prog. Surf. Sci. 27 (1988) 239.
[15] K. Heinz, Vacuum 41 (1990) 328.
[16] Ch. Ammer, Surf. Sci. 287/288 (1993) 964.
[17] J.B. Pendry, J. Phys. C 13 (1980) 937.
[18] G. Meyer, J. Wollschläger and M. Hensler, Surf. Sci. 231 (1990) 64; M. Hensler, Surf. Sci. 298 (1993) 369.
[19] H.A. van der Vegt et al., Phys. Rev. Lett. 68 (1992) 3335.
[20] S. Esch, M. Hohage, T. Michely and G. Comsa, Phys. Rev. Lett. 72 (1994) 518.
[21] G. Rangelov et al., unpublished.
[22] B. Voigtländer et al., Phys. Rev. B 44 (1991) 10354.
[23] R. Bruinsma and A. Zangwill, Phys. Rev. Lett. 55 (1985) 214.
[24] J. de la Figuera et al., Phys. Rev. B 47 (1993) 13043.
[25] J. de la Figuera et al., Phys. Rev. Lett., submitted.
[26] P. Bödeker, A. Abromeit, K. Bröhl, P. Sonntag, N. Metoki and H. Zabel, Phys. Rev. B 47 (1993) 2353.
[27] N. Cabrera and D.A. Vermilyea, The Growth of Crystals from Solutions, Ed. Turnball (Wiley, New York, 1958).
[28] N. Materer, U. Starke, A. Barbieri, R. Döll, K. Heinz, M.A. Van Hove and G.A. Somorjai, Surf. Sci., in press.
[29] J. Camarero, L. Spendeler, G. Schmidt, K. Heinz, J.J. de Miguel and R. Miranda, Phys. Rev. Lett. 73 (1994) 2448.
[30] W.F. Egelhoff and M.T. Kief, Phys. Rev. B 45 (1992) 7795.